

Strain control of composite superconductors to prevent degradation of superconducting magnets due to a quench: II. High-strength, laminated Ag-sheathed Bi-2223 tapes

To cite this article: Tengming Shen *et al* 2018 *Supercond. Sci. Technol.* **31** 015012

Manuscript version: Accepted Manuscript

Accepted Manuscript is “the version of the article accepted for publication including all changes made as a result of the peer review process, and which may also include the addition to the article by IOP Publishing of a header, an article ID, a cover sheet and/or an ‘Accepted Manuscript’ watermark, but excluding any other editing, typesetting or other changes made by IOP Publishing and/or its licensors”

This Accepted Manuscript is © .

During the embargo period (the 12 month period from the publication of the Version of Record of this article), the Accepted Manuscript is fully protected by copyright and cannot be reused or reposted elsewhere.

As the Version of Record of this article is going to be / has been published on a subscription basis, this Accepted Manuscript is available for reuse under a CC BY-NC-ND 3.0 licence after the 12 month embargo period.

After the embargo period, everyone is permitted to use copy and redistribute this article for non-commercial purposes only, provided that they adhere to all the terms of the licence <https://creativecommons.org/licenses/by-nc-nd/3.0>

Although reasonable endeavours have been taken to obtain all necessary permissions from third parties to include their copyrighted content within this article, their full citation and copyright line may not be present in this Accepted Manuscript version. Before using any content from this article, please refer to the Version of Record on IOPscience once published for full citation and copyright details, as permissions will likely be required. All third party content is fully copyright protected, unless specifically stated otherwise in the figure caption in the Version of Record.

View the [article online](#) for updates and enhancements.

10/10/2017, revised version 1

Strain control of composite superconductors to prevent degradation of superconducting magnets due to a quench. II. High-strength, laminated Ag-sheathed Bi-2223 tapes

Tengming Shen^a, Liyang Ye^b, Hugh Higley

Lawrence Berkeley National Laboratory, Berkeley, CA 94720, USA

a. Email: tshen@lbl.gov

b. Now with GE Healthcare

Abstract

In the article I of this series, we described a spiral coil quench technique for probing the influence of the superconductor stress and strain state during normal operation on its margin to degradation during a quench and applied to a Bi-2212 round wire. Here we extend this technique to study failure mechanisms and limits of high-strength Bi-2223 tapes experiencing a quench while carrying a large current in a high magnetic field. In contrast to Bi-2212 magnets made by a wind and react technique for which bending strains can be ignored, Bi-2223 magnets are made with a react and wind technique for which bending strain is significant. The critical tensile stress of Bi-2223 tapes (type HT-NX) decreases from >440 MPa for straight samples to 185 MPa after bent to a diameter D of 50 mm. The quench degradation limit, measured using maximum allowable temperature during a quench $T_{\text{allowable}}$, is greater than 300 K for axial tensile stress $\sigma_a < 94$ MPa; it decreases with increasing tensile axial stress σ_a nonlinearly, dropping to 230 K for $\sigma_a = 125$ MPa. $T_{\text{allowable}}(\sigma_a)$ experimental data at $D=50$ mm is consistently predicted by a general strain model that assumes that quench degradation in NX/Bi-2223 is driven by axial tensile strain in Bi-2223 filaments exceeding the irreversible strain limit. The $T_{\text{allowable}}(\sigma_a)$ is then predicted for various D including $D = 80$ mm important for NMR magnets. The given $T_{\text{allowable}}(D, \sigma_a)$ is easy to use and important for finding the balance between operation stress, and therefore magnetic field generation efficiency, and operation margin when designing a superconducting magnet using Bi-2223 tapes.

10/10/2017, revised version 1

Introduction

Despite being brittle, several superconductors, including Nb₃Sn, Bi-2212, Bi-2223, REBCO, MgB₂, have been arduously developed into the practical form of metal/superconductor composite wire or tape and found or been finding applications in superconducting magnets. Superconductors within high-field magnets must withstand high stresses and a variety of strains resulted from fabrication and operation, which include bending strain due to coil winding, strain due to operational electromagnetic stresses, and thermal strain caused by differential thermal expansion between metal matrix and superconductors during a quench. Determining the true practical conductor limit of superconductors requires to take all of these strains into consideration. Although the mechanical properties of superconductors and the dependence of their critical current density on strains have been studied extensively [1-4], measurements conducted so far evaluate only one or more but not all of these strains seen by superconductors within a magnet. For example, the tensile stress-strain- I_c test using straight samples [1-3] and the I_c -strain tests using hairspring rigs [5, 6] ignore bending strain and thermal strain due to a quench, whereas bending tests doesn't consider strain due to Lorentz force and thermal strain due to a quench [4]. It is understandable that thermal strain due to a quench is rarely considered [7-9] because the failure mechanisms of a superconductor during a quench have yet been determined.

We developed a spiral coil quench technique capable of evaluating all these strains within a test [10]. We have applied it to Bi-2212 round wire, which is made into magnets using a wind-and-react technique that features zero winding strain, to probe the influence of the operational stress and strain state on its margin to degradation during a quench. We found that quench induced degradation for Bi-2212 round wires is driven by axial tensile strain and that the dependence of the margin to degradation during a quench on the operational electromagnetic stresses can be predicted.

Here we extend this technique to study failure mechanisms and limits of high-strength, high-current Bi-2223 tapes, which is made into magnets using a react-and-wind technique that features a large bending strain. The Ag/Bi-2223 tape was the first high- T_c cuprate conductor fabricated into km length conductor with capability to carry high supercurrent, benefiting from the rather simple powder-in-tube fabrication and the invention of the overpressure processing. However, the application of Bi-2223 tapes to high-field magnets had been hampered by low tensile strength due to the necessary use of silver as the matrix. The strength of Ag/Bi-2223 tapes has been improved by laminating them with Cu-alloy or stainless steel tapes. Potential applications of these high-strength, laminated Bi-

10/10/2017, revised version 1

1
2
3 2223 tapes, with MRI, high-field NMR [11], and research superconducting magnets have recently been
4 explored and demonstrated in a 25 T cryogen-free superconducting magnet which includes a 11 T Bi-
5 2223 insert [12], a 20 K, 3 T MRI magnet [13, 14], a 1020 MHz NMR magnet with a 3.6 T Bi-2223 insert
6 coil in series with 20.4 T Nb-Ti and Nb₃Sn outsert coils [15], and a 28 T solenoid [16] [17]. Recently,
7 ultra-high strength, Bi-2223 tapes (“DI-BSCCO™ type HT-NX) became available from Sumitomo
8 Electric Industries (SEI). The tape, laminated with pretensioned Ni-Cr alloy, has a critical tensile
9 strength of greater than 500 MPa at 77 K [18], increasing from about 130 MPa for the type H and type
10 HT conductors that have no mechanical reinforcements [18], and from ~250 MPa for type HT-CA (Cu-
11 alloy laminated) and type HT-SS (stainless steel laminated) conductors [1]. Its critical tensile strain,
12 about 0.55% at 77 K, is also significantly higher than those of the type H and type HT conductors
13 (~0.2%) and type HT-CA and type HT-SS conductors (~0.4%) [1]. Our experiments and analysis are
14 conducted on the type HT-NX tapes.
15
16
17
18
19
20
21
22
23

24 **Methods**

25 *Sample preparation and critical current measurement*

26
27 Samples are commercial ultra-high strength, Bi-2223 tapes (“DI-BSCCO™ type HT-NX) available from
28 SEI and fabricated using a controlled-overpressure (CT-OP) processing. The tape has an average
29 thickness of 0.31 mm and a width of 4.5 mm. It is a 3-ply tape with two Ni-Cr alloy tapes (thickness =
30 30 μm each) soldered to two sides of a type HT Ag/Bi-2223 tape. The temperature and field
31 dependence of its sister wires (“DI-BSCCO™ type H and type HT) $I_c(B,T)$ is given at here ([http://global-
32 sei.com/super/hts_e/type_ht.html](http://global-sei.com/super/hts_e/type_ht.html)) and by Wimbush *et al.* [19]. Its critical bending diameter is around
33 30 mm (95% I_c retention) [20]. Its modulus at 77 K is 90 GPa and its irreversible tensile axial strain is
34 estimated to be 0.55%, measured by tensile stress measurements.
35
36
37
38
39
40
41
42

43 A 1 m of such tape was wound on a G-10 barrel with spiral grooves (50 mm diameter, 5.6 mm pitch
44 length) (Figure 1a). The barrel design is similar to those used for measuring critical current (I_c) of ITER
45 Nb-Ti and ITER Nb₃Sn strands [21]. The critical current was determined using a standard four-point
46 resistive measurement technique with an electric field criterion of 1 μV/cm at 4.2 K and in magnetic
47 fields up to 15 T. The magnetic field was applied parallel to the central axis of the barrel and thus
48 parallel to the tape. During I_c measurements, the transport current is configured such that the Lorentz
49 force pushes the tape against and thus supported by the G-10 barrel and experiences zero hoop stress
50 (Figure 1b).
51
52
53
54
55
56
57
58
59
60

10/10/2017, revised version 1

Determining the critical axial tensile stress using hoop stress

The critical axial stress at which I_c degrades irreversibly is an important engineering parameter and was determined using the spiral coil as follows. The spiral coil technique allows a hoop stress induced using a transport current oriented such that the Lorentz force was outward away from the G-10 barrel ($\sigma_h = B Jr$, where J is the current density averaged over the entire wire cross-section and r the radius of the spiral. Figure 1c). The transport critical current was re-measured after applying the hoop stress.

Quench behaviors investigation

The coil was also instrumented with a heater for inducing a quench, and voltage taps and thermocouples for monitoring quench propagation (Figure 2a and 2c). The heater is an epoxy spot heater (Ecobond 60L) designed for triggering small normal zones and it is also easy to mount onto the sample. The normal zone evolution was monitored via thermocouples (E-type, AWG32) and voltage taps around the hot zone. The hot spot temperature was obtained by cross-examining the measured resistivity of the hot zone with the temperature dependence of Bi-2223 wire resistivity and verified by thermocouples. A typical sequence of voltage signal development after a quench is shown in Figure 2b.

Determining the maximum allowable temperature during a quench, $T_{\text{allowable}}$, with increasing axial stress

The spiral coil geometry lends itself well to simulating a quench with a large current in high magnetic field and thus large Lorentz forces. This is accomplished by applying a controlled hoop stress and initiating a quench using a heater, similar to previous studies on short straight samples and coils. Samples were quenched with raising hot spot temperature incrementally, beginning around 50 K, and after each quench, the I_c of the sample was re-measured with zero hoop stress. The safety margin was measured using the maximum allowable hot spot temperature $T_{\text{allowable}}$ during a quench, which is defined as the hot spot temperature at which I_c of the wire degrades by 5%. This experiment is representative of quenches in high-field magnets.

Results

$I_c(B)$ and n -value

Figure 3 presents $I_c(B)$ and n -values of two barrel samples, confirming high I_c and n -values of this material for practical magnet applications. Samples show high strong hysteresis in I_c , with I_c measured at decreasing field being significantly higher than I_c measured at ascending field.

10/10/2017, revised version 1

Axial tensile stress limit for D=50 mm

Figure 4 presents l_c with increasing axial stress for a barrel with $D=50$ mm. l_c shows irreversible degradation ($l_c(\text{after stress})/\text{initial } l_c \leq 0.99$) with axial stress greater than 150 MPa, and at 185 MPa, loses 5% of its original l_c . The axial stress limit found is significantly lower than the values measured from tensile tests of straight samples.

Stress dependence of maximum allowable temperature during a quench $T_{allowable}(\sigma_a)$ for D=50 mm

Figure 5 presents results of quench experiments with or without (safe mode) hoop stress at 4.2 K and 15 T. Without hoop stress and with hoop stress smaller than 94 MPa, samples survive hot spot temperature greater than 300 K (Q5, sample #1) whereas under a hoop stress of 121 MPa, the maximum allowable temperature during a quench, $T_{allowable}$, decreases to 232 K. Figure 6 presents $T_{allowable}$ as a function of applied stress, showing the clear trend of the decrease of $T_{allowable}$ with increasing axial stress.

Quench induced degradation behaviors

Figure 7 presents a typical quench degradation behavior. The degradation rather localized due to slow normal zone propagation. Similar to Bi-2212, the degradation correlates with the local hot spot temperature T_{max} well.

Analysis and discussion

Failure analysis

In composite superconducting wires the total axial strain of superconductor filaments in a composite superconductors, ϵ_t , during a quench can be described as

$$\epsilon_t = \epsilon_b + \epsilon_L + \epsilon_q \quad (1)$$

where ϵ_b is the bending strain, ϵ_L the strain due to Lorentz forces, and ϵ_q the axial tensile strain from differential thermal expansion between the entire wire and the superconductor filaments due to the temperature rise during the quench. For this experiment, $\epsilon_b = 0.32\%$ for $D = 50$ mm (given by $\epsilon_b = \frac{2 \cdot t}{D}$, where t is the distance of the outermost Bi-2223 filaments away from the central bending plane.

Here $t=0.08$ mm.), and $\epsilon_L = \epsilon_h$, which is the hoop strain (given by $\epsilon_h = \frac{\sigma_h}{E}$, where E is the modulus of HT-NX Bi-2223. Here $E=90$ GPa). Assuming that that ϵ_q relates to T_{max} only and does not relate to

10/10/2017, revised version 1

either temperature rise rate dT_{\max}/dt or temperature gradient dT_{\max}/dx , ϵ_q in the Bi-2223 filaments can be appropriated by,

$$\epsilon_q |_{\text{Bi-2223 filaments}} = \Delta L / L_{T_{\max}-4.2 K} |_{\text{wire}} - \Delta L / L_{T_{\max}-4.2 K} |_{\text{Bi-2223 filaments}} \quad (2)$$

where $\Delta L / L_{T_{\max}-4.2 K} |_{\text{Bi-2223 HT-NX tape}}$ and $\Delta L / L_{T_{\max}-4.2 K} |_{\text{Bi-2223 filaments}}$ the total linear expansion from 4.2 K to T_{\max} for the entire wire and the Bi-2223 filaments, respectively. As a reference, $\Delta L / L_{300 K-4.2 K} |_{\text{wire}} = 0.31\%$ whereas $\Delta L / L_{300 K-4.2 K} |_{\text{Bi-2223 filaments}} = 0.16\%$ [22].

Figure 8 plots the total axial strain applied to the Bi-2223 filaments, including ϵ_h and ϵ_q for cases A-E in Figure 4. The failure limits shown are remarkably consistent among all cases: At a total axial strain of 0.52-0.55%, I_c of Bi-2223 conductors degrades irreversibly.

The implications of Figure 8 are strong. First, it shows that the failure during a quench for Bi-2223 conductor is driven by axial tensile strain in Bi-2223 filaments and occurs when their axial strain exceeds the measured irreversible tensile strain limit. Second, both bending strain and quench induced thermal strain manifest themselves as axial strains that can be simply be added into the total axial strain. Therefore, it is rather simple to predict the failure limits of Bi-2223 conductors, including the type H, type HT, type HT-SS, type HT-CA, and type HT-NX during a quench.

Failure limit prediction

Based on these new findings, Figure 9 predicts failure limits of Bi-2223 as a function of bending diameter D when there is no quench ($\sigma_c = E \cdot \epsilon'_c = E \cdot (\epsilon_c - \epsilon_b)$, where ϵ'_c is the modified irreversible tensile axial strain with bending strain $\epsilon_b = \frac{2 \cdot t}{D}$ taken into consideration). Critical tensile stress σ_c decreases with bending diameter D , dropping to ~ 300 MPa with $D = 80$ mm, and ~ 200 MPa with $D = 50$ mm. The prediction is consistent with this experiment and $\sigma_c = 400$ MPa at $D = 108$ mm found by Miyoshi *et al.* [23].

Figure 10 predicts failure limits of Bi-2223 as a function of bending diameter D when there is a quench, expressed as $T_{\text{allowable}}(D, \sigma_a)$ ($\sigma_a = \sigma_h$ in this case). This plot has important engineering values because it defines the practical limits of Bi-2223 conductors. At $D = 80$ mm which is required by NMR magnets, to keep $T_{\text{allowable}} > 300$ K, the hoop stress applied should not exceed 200 MPa. From this plot, it is clear that the design of this 25 T magnet [8, 12] ($D = 95.8$ mm, $\sigma_h = 323$ MPa; $T_{\text{allowable}} = 200$ K according to Figure 10) is too aggressive, as it likely fails during quenches if the maximum temperature during a quench exceeds 200 K. The plot is easy to use as $T_{\text{allowable}}$ can be correlated to current density in Ag

10/10/2017, revised version 1

1
2
3 matrix J_m , and quench protection parameters including t_s , the time between a quench occurring and
4 the magnet current decaying, and t_D , the time constant of magnet current decay through a simple
5 adiabatic heat transfer analysis.
6
7

8
9 Our $T_{\text{allowable}}(D, \sigma_a)$ predication is a conservative limit for using Bi-2223 type HT-NX conductor for
10 several reasons. σ_h decreases, increasing $T_{\text{allowable}}$, if a quench is detected and magnet current is
11 forced to decay. Moreover, in a solenoid, the highest hoop stress is not necessarily at the innermost
12 layer, where the bending strain is most significant and the field is strongest.
13
14

15 16 *Other failure mechanisms*

17
18 One of the samples also failed with N-Cr-alloy buckling due to a quench and delaminating from Ag/Bi-
19 2223 tape. These additional failure mechanisms are likely a characteristics shared by all laminated Bi-
20 2223 conductors.
21
22

23 24 **Conclusions**

25
26 We extend a new spiral coil quench technique to explore practical engineering limits of an ultra-high
27 strength, high-current Bi-2223 tape. Our experiments show that failures of Bi-2223, like Bi-2212 wires,
28 during a quench is driven by axial tensile strain. Our analysis show that the experimental results can
29 be predicted using a simple strain analysis. We further extended the analysis to predict the maximum
30 allowable temperature during a quench $T_{\text{allowable}}(D, \sigma_a)$ at various bending diameters. The conductor
31 degrades permanently above $T_{\text{allowable}}$. The resulted plot is easy to use and has significant engineering
32 values for designing magnets using Bi-2223 conductors.
33
34
35
36
37
38

39 **Acknowledgements**

40
41 This work was funded by the Office of High Energy Physics of the U.S. Department of Energy (DOE) through a US
42 DOE Early Career Award. Work at Lawrence Berkeley National Lab was supported by the Director, Office of
43 Science, Office of High Energy Physics, of the U.S. Department of Energy under Contract No. DE-AC02-
44 05CH11231. We thank Arno Godeke and Scott Marshall with the National High Magnetic Field Laboratory for
45 supplying conductors used in this study.
46
47
48

49 **REFERENCES**

- 50
51
52 [1] N. Ayai, K. Yamazaki, M. Kikuchi, G. Osabe, H. Takaaze, H. Takayama, *et al.*, "Electrical and mechanical
53 properties of DI-BSCCO type HT reinforced with metallic sheathes," *IEEE Trans. Appl. Supercond.*, vol.
54 19, pp. 3014-3017, 2009.
55 [2] M. Sugano, K. Osamura, and M. Hojo, "Mechanical properties of Bi2223 filaments extracted from
56 multifilamentary tape evaluated by the single-fibre tensile test," *Supercond. Sci. and Technol.*, vol. 16,
57 p. 571, 2003.
58
59
60

10/10/2017, revised version 1

- 1
2
3
4
5
6
7
8
9
10
11
12
13
14
15
16
17
18
19
20
21
22
23
24
25
26
27
28
29
30
31
32
33
34
35
36
37
38
39
40
41
42
43
44
45
46
47
48
49
50
51
52
53
54
55
56
57
58
59
60
- [3] P. Sunwong, J. S. Higgins, and D. P. Hampshire, "Angular, temperature, and strain dependencies of the critical current of DI-BSCCO tapes in high magnetic fields," *IEEE Trans. Appl. Supercond.*, vol. 21, pp. 2840-2844, 2011.
- [4] H.-S. Shin and K. Katagiri, "Critical current degradation behaviour in Bi-2223 superconducting tapes under bending and torsion strains," *Supercond. Sci. and Technol.*, vol. 16, p. 1012, 2003.
- [5] H. Kitaguchi, K. Itoh, H. Kumakura, T. Takeuchi, K. Togano, and H. Wada, "Strain effect in Bi-based oxide/Ag superconducting tapes," *IEEE Trans. Appl. Supercond.*, vol. 11, pp. 3058-3061, 2001.
- [6] B. ten Haken, A. Beuink, and H. H. ten Kate, "Small and repetitive axial strain reducing the critical current in BSCCO/Ag superconductors," *IEEE Trans. Appl. Supercond.*, vol. 7, pp. 2034-2037, 1997.
- [7] S. Hahn, J. Bascunán, W. Yao, and Y. Iwasa, "Two HTS options for a 600MHz insert of a 1.3 GHz LTS/HTS NMR magnet: YBCO and BSCCO," *Physica C*, vol. 470, pp. 1721-1726, 2010.
- [8] S. Hanai, T. Tsuchihashi, S. Ioka, K. Watanabe, S. Awaji, and H. Oguro, "Development of an 11 T BSCCO Insert Coil for a 25 T Cryogen-free Superconducting Magnet," *IEEE Trans. Appl. Supercond.*, vol. 27, p. 4602406, 2017.
- [9] Y. Yanagisawa, Y. Xu, S. Iguchi, M. Hamada, S. Matsumoto, G. Nishijima, *et al.*, "Combination of high hoop stress tolerance and a small screening current-induced field for an advanced Bi-2223 conductor coil at 4.2 K in an external field," *Supercond. Sci. and Technol.*, vol. 28, p. 125005, 2015.
- [10] L. Ye, P. Li, J. Jaroszynski, J. Schwartz, and T. Shen, "Strain control of composite superconductors to prevent degradation of superconducting magnets due to a quench: I. Ag/Bi₂Sr₂CaCu₂O_x multifilament round wires," *Supercond. Sci. and Technol.*, vol. 30, p. 025005, 2016.
- [11] W. Marshall, M. Bird, A. Godeke, D. Larbalestier, W. Markiewicz, and J. White, "Bi-2223 Test Coils for High-Resolution NMR Magnets," *IEEE Trans. Appl. Supercond.*, vol. 27, p. 4300905, 2017.
- [12] S. Awaji, K. Watanabe, H. Oguro, H. Miyazaki, S. Hanai, T. Tosaka, *et al.*, "First performance test of a 25 T cryogen-free superconducting magnet," *Supercond. Sci. and Technol.*, vol. 30, p. 065001, 2017.
- [13] Y. Terao, O. Ozaki, C. Ichihara, S. Kawashima, T. Hase, H. Kitaguchi, *et al.*, "Newly designed 3 T MRI magnet wound with Bi-2223 tape conductors," *IEEE Trans. Appl. Supercond.*, vol. 23, pp. 4400904-4400904, 2013.
- [14] H. Kitaguchi, O. Ozaki, T. Miyazaki, N. Ayai, K.-i. Sato, S.-i. Urayama, *et al.*, "Development of a Bi-2223 HTS magnet for 3T MRI system for human brains," *IEEE Trans. Appl. Supercond.*, vol. 20, pp. 710-713, 2010.
- [15] K. Hashi, S. Ohki, S. Matsumoto, G. Nishijima, A. Goto, K. Deguchi, *et al.*, "Achievement of 1020 MHz NMR," *J Magn. Reson.*, vol. 256, pp. 30-33, 2015.
- [16] K. Kajita, S. Iguchi, Y. Xu, M. Nawa, M. Hamada, T. Takao, *et al.*, "Degradation of a REBCO Coil due to cleavage and peeling originating from an electromagnetic force," *IEEE Trans. Appl. Supercond.*, vol. 26, pp. 1-6, 2016.
- [17] H. Maeda, T. Yamazaki, Y. Nishiyama, M. Hamada, K. Hashi, T. Shimizu, *et al.*, "Development of Super-High-Field NMR Operated Beyond 1 GHz Using High-Temperature Superconducting Coils," *eMagRes*, vol. 5, p. 1109, 2016.
- [18] A. Godeke, D. Abaimov, E. Arroyo, N. Barrett, M. Bird, A. Francis, *et al.*, "A Feasibility Study of High-Strength Bi-2223 Conductor for High-Field Solenoids," *Supercond. Sci. and Technol.*, 2016.
- [19] S. C. Wimbush, N. M. Strickland, and N. J. Long, "Low-Temperature Scaling of the Critical Current in 1 G HTS Wires," *IEEE Trans. Appl. Supercond.*, vol. 25, pp. 1-5, 2015.
- [20] T. Nakashima, K. Yamazaki, S. Kobayashi, T. Kagiya, M. Kikuchi, S. Takeda, *et al.*, "Drastic improvement in mechanical properties of DI-BSCCO wire with novel lamination material," *IEEE Trans. Appl. Supercond.*, vol. 25, pp. 1-5, 2015.
- [21] I. Pong, M. Jewell, B. Bordini, L. Oberli, S. Liu, F. Long, *et al.*, "Worldwide benchmarking of ITER internal tin and NbTi strands test facilities," *IEEE Trans. Appl. Supercond.*, vol. 22, pp. 4802606-4802606, 2012.
- [22] J. Ekin, *Experimental Techniques for Low-Temperature Measurements: Cryostat Design, Material Properties and Superconductor Critical-Current Testing*: OUP Oxford, 2006.
- [23] Y. Miyoshi, G. Nishijima, H. Kitaguchi, and X. Chaud, "Hoop stress test on new high strength alloy laminated Bi-2223 conductor," *Supercond. Sci. and Technol.*, vol. 28, p. 075013, 2015.

10/10/2017, revised version 1

List of Figures

Figure 1: (a) A photo of a Bi-2223 spiral coil mounted on a G-10 barrel, (b) illustration of the safe mode for I_c measurement, (c) illustration of the hoop stress mode for investigating conductor limits.

Figure 2: (a) Schematics of instrumentation used for the heater-induced quench experiment (for V_0 , V_{L1} , V_{L2} , V_{L3} , V_{R1} , V_{R2} , V_{R3} , tap lengths are 1 cm.), (b) typical $V(t)$ during a quench of Bi-2223 HT-NX tape, (c) A photo of a Bi-2223 spiral coil, instrumented with voltage taps (VT = voltage tap) and thermocouples, mounted on the test probe. TC=thermocouple; VT=voltage tap.

Figure 3: $I_c(B)$ and n-value of the Bi-2223 tapes at 4.2 K in ascending and descending magnetic field.

Figure 4: I_c at 4.2 K and 15 T for HT-NX Bi-2223 tapes ($D=50$ mm) with increasing Lorentz force applied. I_c was measured without hoop stresses after each force cycle.

Figure 5: Record of I_c and maximum hot spot temperature T_{max} for quench experiments performed on (a) sample #1, and (b) sample #2.

Figure 6: Maximum allowable temperature $T_{allowable}$ during a quench as a function of hoop stress σ_h applied for HT-NX Bi-2223 tape ($D=50$ mm).

Figure 7: An example of quench induced I_c distribution and associated hot spot temperature distribution after a quench (Q17 for sample #1.).

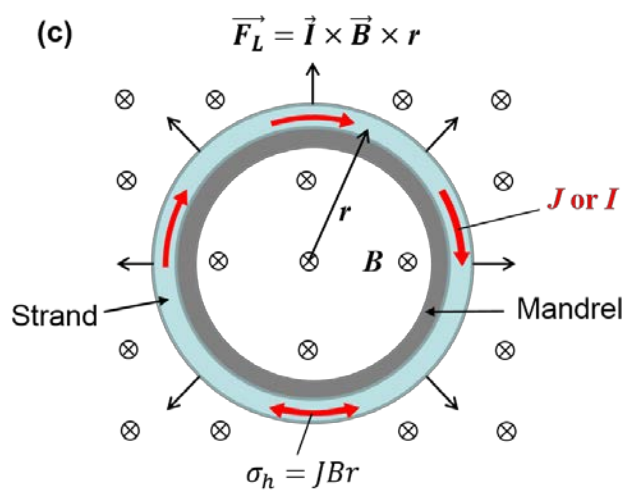
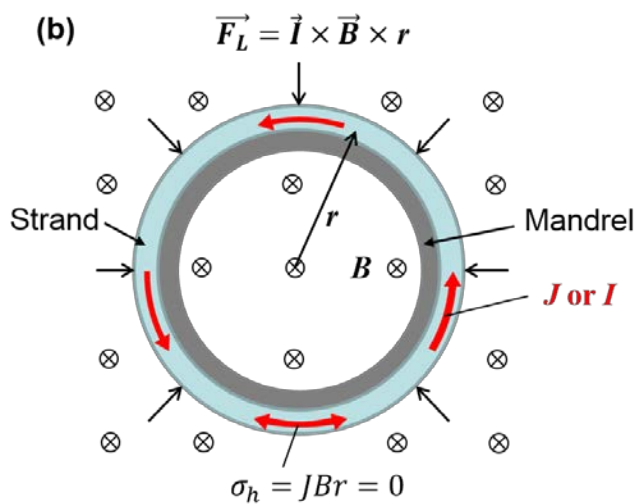
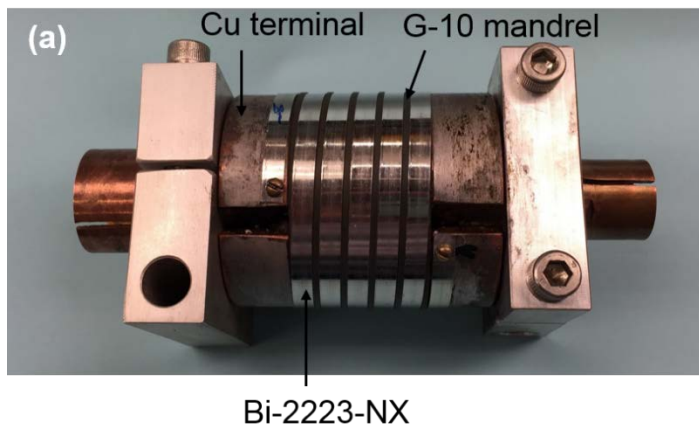
Figure 8: Strain seen by the Bi-2223 filaments for quenches and non-quench scenario presented in Figure 4.

Figure 9: Predicted critical tensile stress as a function of bending diameter D for Bi-2223 HT-NX.

Figure 10: Maximum allowable temperature $T_{allowable}$ during a quench as a function of hoop stress σ_h applied for HT-NX Bi-2223 tape with various bending diameter.

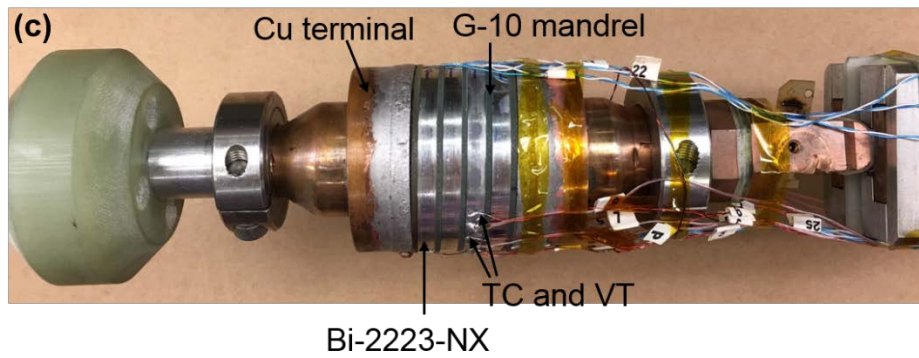
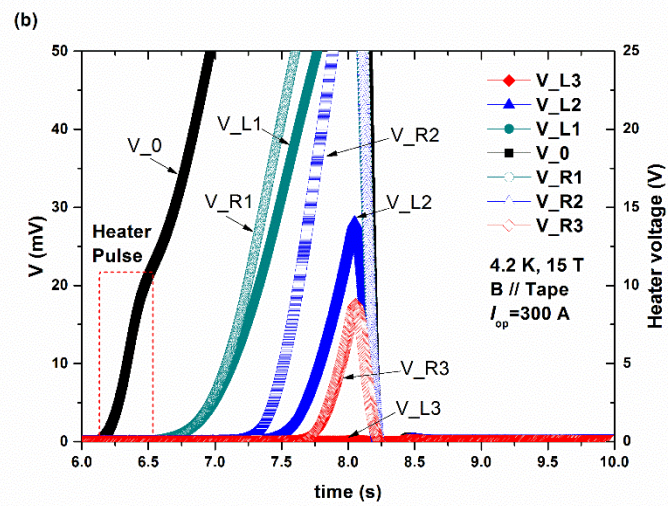
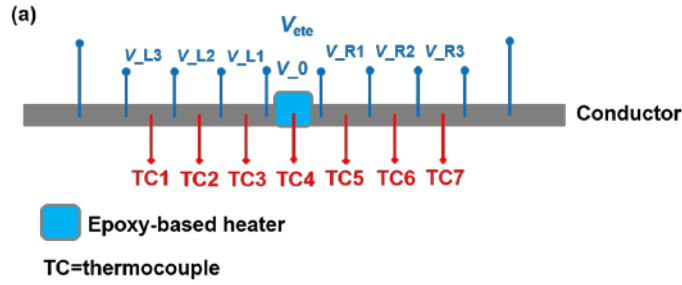
10/10/2017, revised version 1

Figure 1:



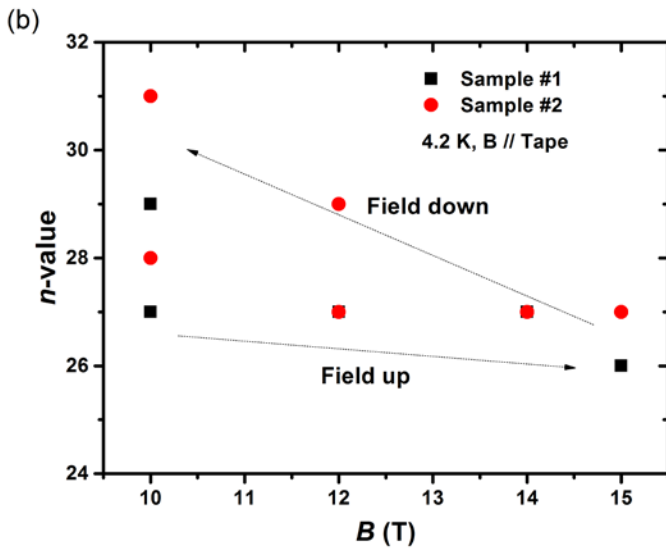
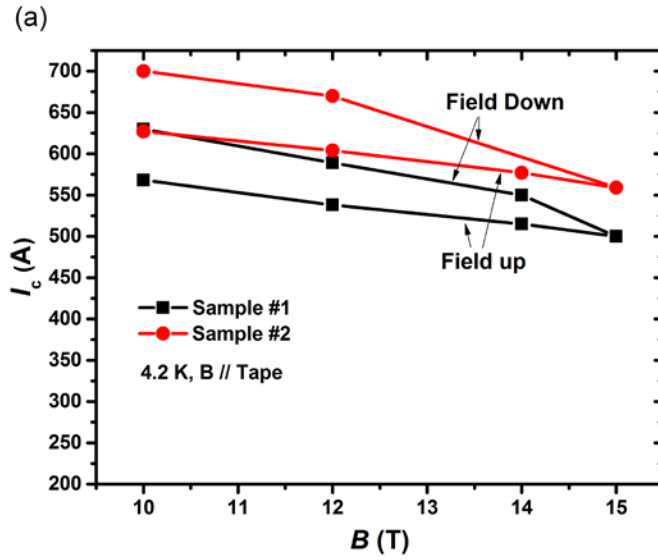
10/10/2017, revised version 1

Figure 2:



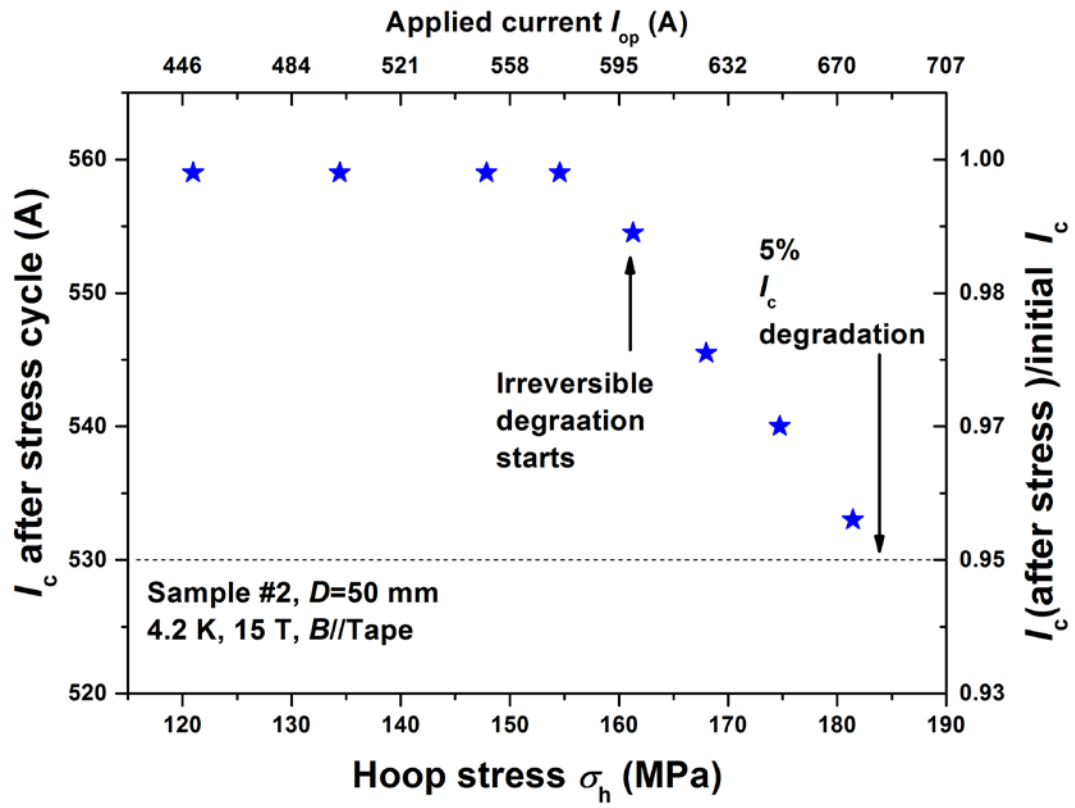
10/10/2017, revised version 1

Figure 3:



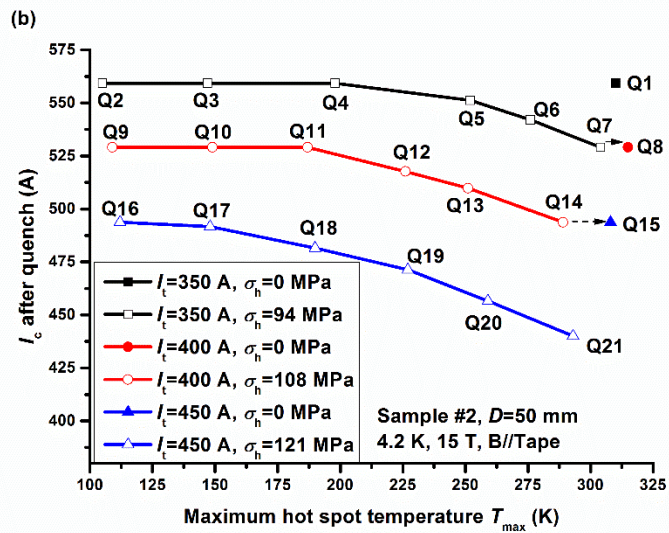
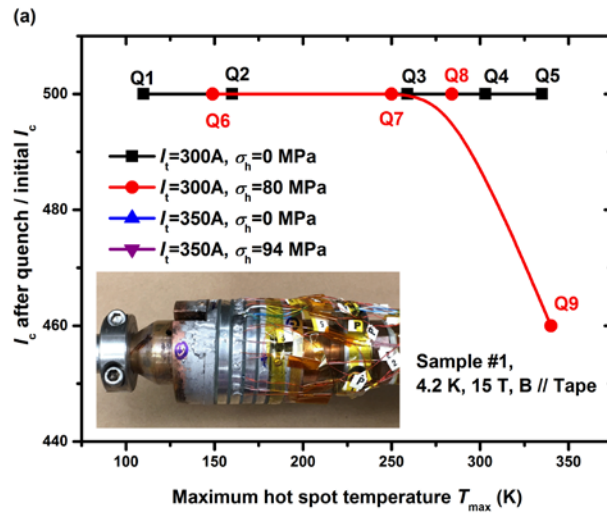
10/10/2017, revised version 1

Figure 4:



10/10/2017, revised version 1

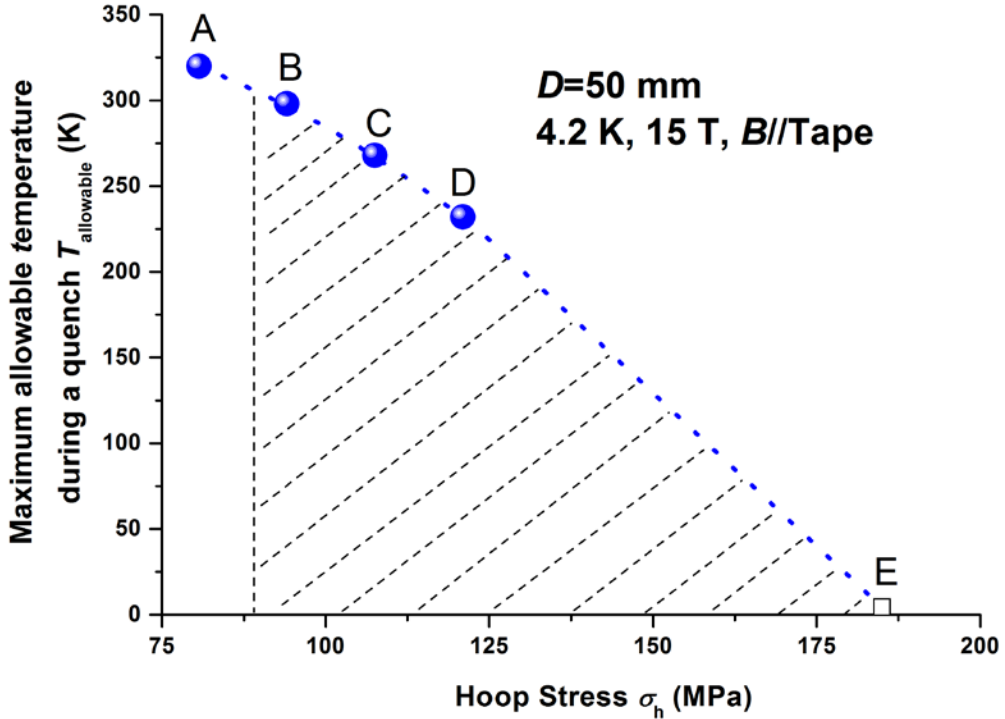
Figure 5



10/10/2017, revised version 1

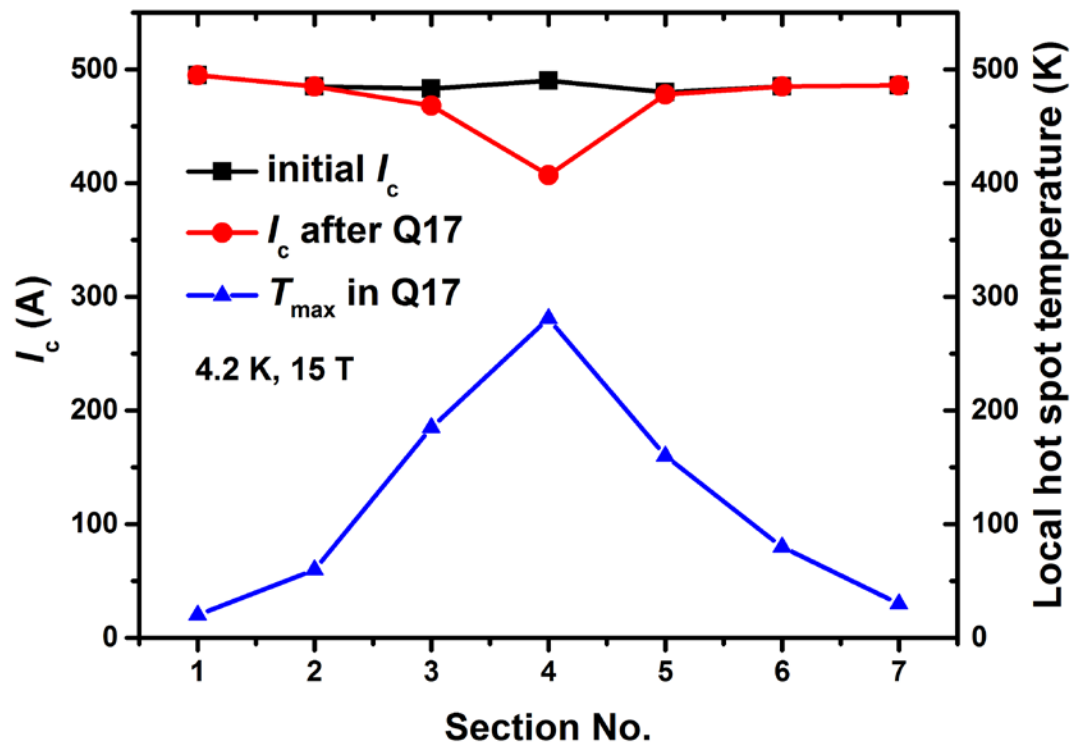
1
2
3
4
5
6
7
8
9
10
11
12
13
14
15
16
17
18
19
20
21
22
23
24
25
26
27
28
29
30
31
32
33
34
35
36
37
38
39
40
41
42
43
44
45
46
47
48
49
50
51
52
53
54
55
56
57
58
59
60

Figure 6:



10/10/2017, revised version 1

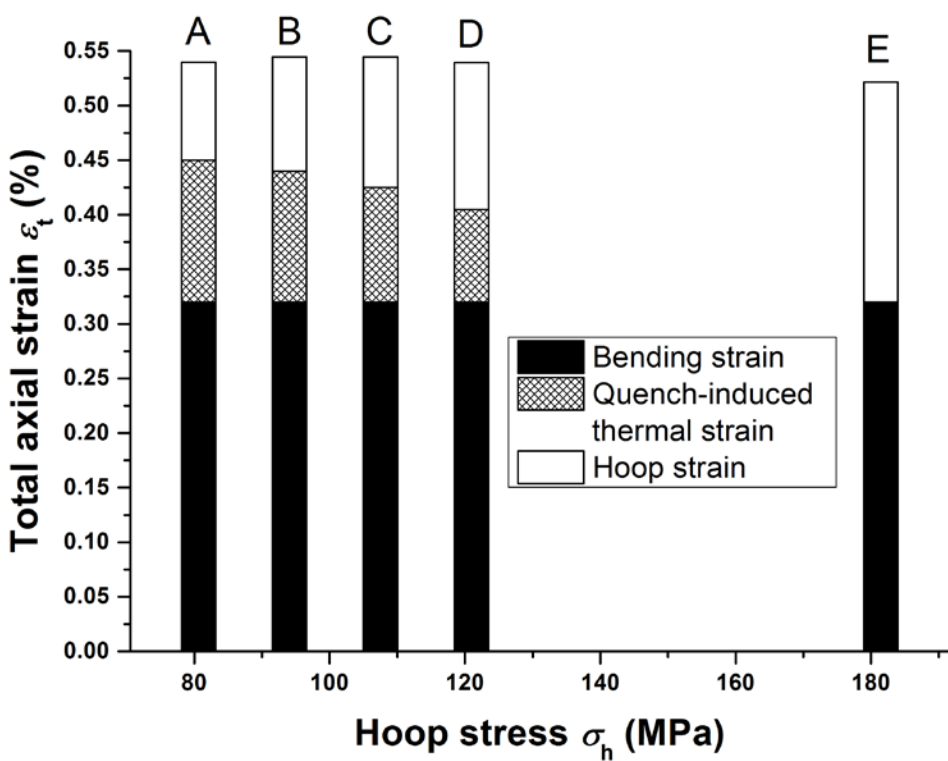
Figure 7:



10/10/2017, revised version 1

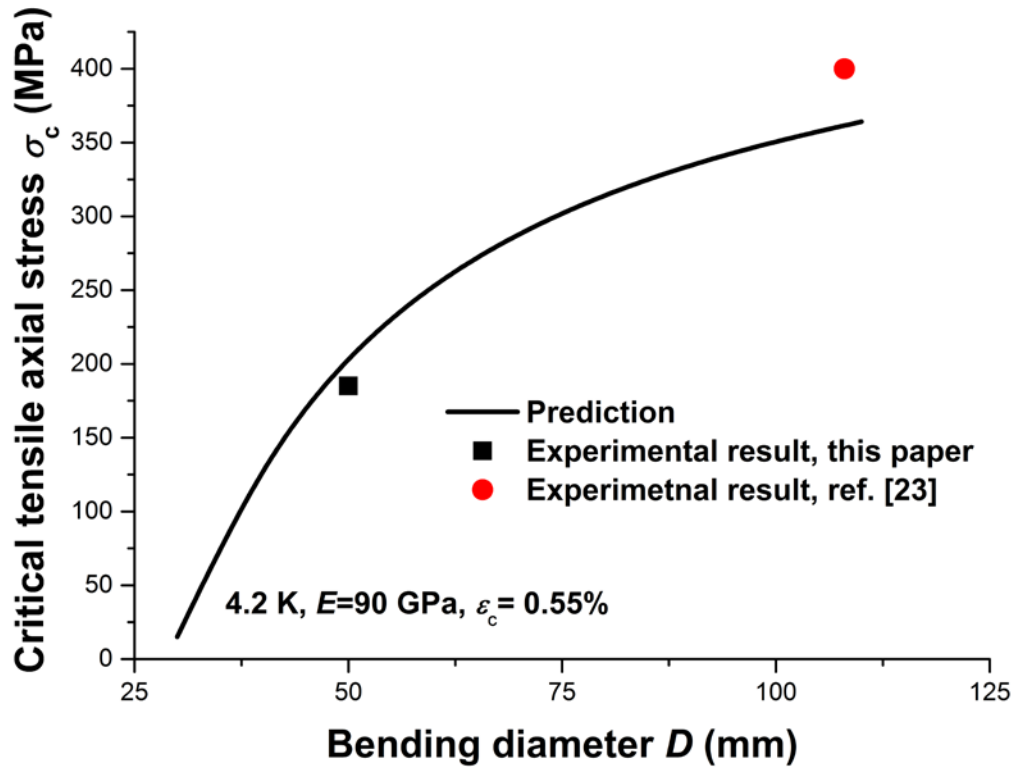
1
2
3
4
5
6
7
8
9
10
11
12
13
14
15
16
17
18
19
20
21
22
23
24
25
26
27
28
29
30
31
32
33
34
35
36
37
38
39
40
41
42
43
44
45
46
47
48
49
50
51
52
53
54
55
56
57
58
59
60

Figure 8:



10/10/2017, revised version 1

Figure 9:



10/10/2017, revised version 1

1
2
3
4
5
6
7
8
9
10
11
12
13
14
15
16
17
18
19
20
21
22
23
24
25
26
27
28
29
30
31
32
33
34
35
36
37
38
39
40
41
42
43
44
45
46
47
48
49
50
51
52
53
54
55
56
57
58
59
60

Figure 10:

